

Oleocanthal Enhances Amyloid- β Clearance from the Brains of TgSwDI Mice and in Vitro across a Human Blood-Brain Barrier Model

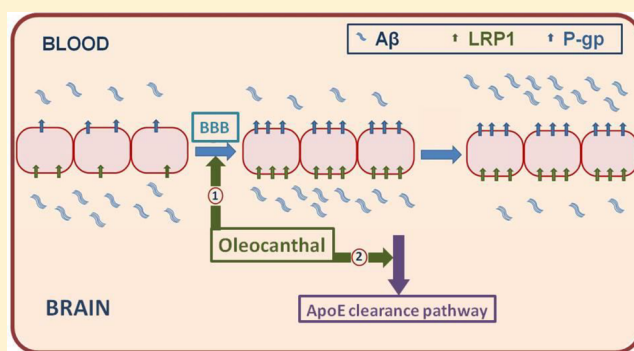
Hisham Qosa,^{†,§} Yazan S. Batarseh,^{†,§} Mohamed M. Mohyeldin,[†] Khalid A. El Sayed,[†] Jeffrey N. Keller,[‡] and Amal Kaddoumi^{*,†}

[†]Department of Basic Pharmaceutical Sciences, School of Pharmacy, University of Louisiana at Monroe, Monroe, Louisiana 71201, United States

[‡]Pennington Biomedical Research Center, Louisiana State University, Baton Rouge, Louisiana 70803, United States

ABSTRACT: Numerous clinical and preclinical studies have suggested several health promoting effects for the dietary consumption of extra-virgin olive oil (EVOO) that could protect and decrease the risk of developing Alzheimer's disease (AD). Moreover, recent studies have linked this protective effect to oleocanthal, a phenolic secoiridoid component of EVOO. This protective effect of oleocanthal against AD has been related to its ability to prevent amyloid- β ($A\beta$) and tau aggregation in vitro, and enhance $A\beta$ clearance from the brains of wild type mice in vivo; however, its effect in a mouse model of AD is not known. In the current study, we investigated the effect of oleocanthal on pathological hallmarks of AD in TgSwDI, an animal model of AD. Mice treatment for 4 weeks with oleocanthal significantly decreased amyloid load in the hippocampal parenchyma and microvessels. This reduction was associated with enhanced cerebral clearance of $A\beta$ across the blood-brain barrier (BBB). Further mechanistic studies demonstrated oleocanthal to increase the expression of important amyloid clearance proteins at the BBB including P-glycoprotein and LRP1, and to activate the ApoE-dependent amyloid clearance pathway in the mice brains. The anti-inflammatory effect of oleocanthal in the brains of these mice was also obvious where it was able to reduce astrocytes activation and IL-1 β levels. Finally, we could recapitulate the observed protective effect of oleocanthal in an in vitro human-based model, which could argue against species difference in response to oleocanthal. In conclusion, findings from in vivo and in vitro studies provide further support for the protective effect of oleocanthal against the progression of AD.

KEYWORDS: Alzheimer's diseases, amyloid- β , blood-brain barrier, clearance, oleocanthal



Mediterranean diet is considered one of the most important healthy habits of the Mediterranean population. Emerging evidence from clinical studies has correlated Mediterranean diets to the low risk of several noncommunicable diseases such as cardiovascular disease and certain types of cancers.^{1–3} Moreover, a very recent study reported that nutrition intervention with Mediterranean diet to significantly improve the participants' cognitive performance.⁴ Mediterranean diet contains several elements that were evaluated for their health promoting effect.^{5,6} Extra-virgin olive oil (EVOO) is one of the characteristic elements of Mediterranean diet that has been extensively studied for its potential health promoting activities.^{5,7} Several clinical studies have shown the enrichment of Mediterranean diet with EVOO to improve cognitive performance and slow the progression of memory impairment.^{3,4,8,9} EVOO is defined as a high quality olive oil that is obtained from the first pressing of olive fruit by mechanical means (European Commission, 2003). EVOO has long been recognized for its extraordinary fat content, which is composed of two fractions, the glycerol (~95%) and nonglycerol (~5%) fractions.¹⁰ About 75% of fat content of EVOO (in its glycerol

fraction) is in the form of oleic acid (a monounsaturated, omega-9 fatty acid) that was previously reported to improve cardiovascular functions such as reduction in blood cholesterol and blood pressure.¹¹ The nonglycerol fraction contains phenolic compounds that account for EVOO resistance to oxidative rancidity.¹² Most of EVOO phenolic compounds are antioxidant molecules that are able to counter the toxic effects of oxygen metabolism such as free radical formation, thus protecting cells against oxidative damage.^{13,14} The total nonglycerol content of EVOO is about 500 mg/kg and includes over 30 chemical substances belonging to different classes, such as alcohols, sterols, hydrocarbons, and volatile compounds.⁵ The most abundant phenolic compounds in EVOO are tyrosol, hydroxytyrosol, and other complex ester secoiridoids, which share the hydroxytyrosol or tyrosol alcohol moiety. Among EVOO phenolics, *S*(-)-oleocanthal, a dialdehydic form of (-)-deacetyxylogstroside glycoside, is a

Received: July 10, 2015

Revised: September 7, 2015

Published: September 8, 2015

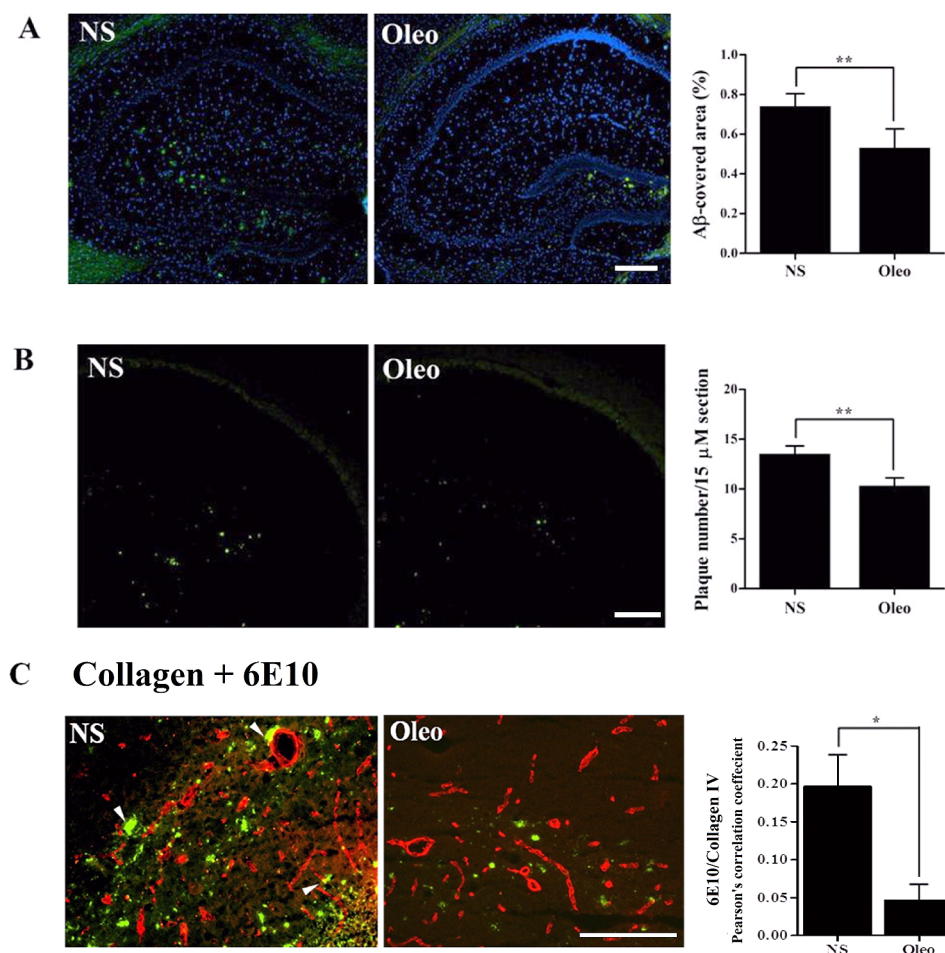


Figure 1. Oleocanthal (Oleo) treatment reduces A β burden in the hippocampus of TgSwDI. (A) Representative hippocampus sections stained with 6E10 (green) antibody against A β to detect A β load and DAPI (blue) to stain nuclei. (B) Representative hippocampus sections stained with thioflavin-S to detect A β -plaque burden. Quantitative analysis of total A β load (A) and A β plaque load (B) showed a significant reduction in A β load (measured as % of A β -covered area) and A β plaque load (measured as number of plaques per 15 μ m section) in the hippocampus of Oleo treatment group. (C) Double-immunostaining for the colocalization of A β (6E10, green) and brain microvessels (collagen-IV, red) showed a significant reduction in Pearson's correlation coefficient between A β and microvessels in Oleo treated group. Arrows indicate the presence of vascular deposition of A β in normal saline (NS) group but not in oleocanthal treated group. TgSwDI mice were treated with oleocanthal (5 mg/kg/day intraperitoneally) or NS for 4 weeks beginning at age 4 months. Data is presented as mean \pm SEM of 6 mice in each group with 18 sections/mouse (* P < 0.05 and ** P < 0.01). Scale bar, 50 μ m.

naturally occurring phenolic secoiridoid that has related chemical structure to the secoiridoids ligstroside and oleuropein aglycones, which are common in EVOO. Oleocanthal is responsible for the bitter and pungent taste of EVOO, and has anti-inflammatory and antioxidant properties similar to the nonsteroidal anti-inflammatory drug ibuprofen.¹⁵

Several animal and in vitro studies have shown that oleocanthal and phenolic compounds of EVOO possess important neuroprotective activities against Alzheimer's disease (AD).^{16–20} In vitro studies with oleocanthal demonstrated its effect on the key mediators of AD pathogenesis, amyloid- β (A β) and hyperphosphorylated tau proteins,^{16,21,22} which contribute significantly to neurodegeneration and memory loss.²³ In these studies, oleocanthal prevented the aggregation of hyperphosphorylated tau by locking tau into the naturally unfolded state,²¹ and altered the oligomerization state of soluble A β_{42} oligomers that protected neurons from their synaptopathological effect.²² In addition, we recently showed the ability of oleocanthal to enhance cerebrovascular clearance of exogenous A β across the blood-brain barrier (BBB) of wild type mice brains.¹⁶

While previous in vitro studies and our in vivo study in wild type mice provided insights on the mechanisms of oleocanthal neuroprotective activity, none of these studies tested the reported beneficial effects of oleocanthal in an AD model. Therefore, in the current study, we examined the effect of oleocanthal on A β load in the brain parenchyma of a mouse model of AD, namely, TgSwDI mice, and on A β deposit on brain microvessels. In addition, the effect of oleocanthal on cerebral clearance and production of A β , tau hyperphosphorylation and its anti-inflammatory effect on astrocytes and brain inflammatory cytokines release were investigated. To test whether the observed effects in the mouse model could be extended to humans, we studied the effect of oleocanthal on A β clearance and production using a cell-based in vitro model.

RESULTS AND DISCUSSION

Previous clinical and preclinical studies suggested EVOO and its phenolic constituent, oleocanthal, have several health promoting effects that could protect and decrease the risk of AD.^{8,9,24,25} Understanding the mechanisms by which oleocan-

thal, as a natural small molecule, protects against AD will be of great importance particularly due to the dramatic rise in AD prevalence and the lack of options for its effective treatment. Several mechanisms have been postulated for oleocanthal protective effect against AD such as inhibition of $A\beta$ and tau aggregation supported by in vitro results and enhancement of stereotaxically microinjected $A\beta$ clearance across the BBB of wild-type mice.^{16,21,22} However, none of these studies tested the protective effect of oleocanthal in a model of AD. In the present study, we investigated the effects of oleocanthal treatment on $A\beta$ - and tau- related pathological alterations that are associated with the progression of AD in TgSwDI mice. Moreover, we studied the effect of oleocanthal treatment on $A\beta$ production and clearance in a representative human-based in vitro model.

In AD, memory deficits associated with disease progression are likely to result from pathological changes in the entorhinal cortex and hippocampus; both regions are critical for formation of new memories and among the most severely affected in AD.^{23,26,27} In addition, it has been suggested that hippocampal $A\beta$ deposition reflects the selective vulnerability of this region for AD pathogenesis.²⁷ Therefore, reduction of $A\beta$ load in the hippocampus is considered one of the main therapeutic aims in the treatment of AD; hence, in the current study, we monitored changes in $A\beta$ load in the hippocampus region of TgSwDI mice brains. At an early age, these mice exhibit low levels of soluble $A\beta_{40}$ and $A\beta_{42}$ in their brains, and the levels increase significantly by 12 months. However, the soluble fraction continues to represent a very small fraction of the insoluble $A\beta$ peptides.²⁸ Due to this low level of soluble $A\beta$ peptides in the mouse brain at the age of 5 months (at end of treatment), total $A\beta$ levels were determined by immunostaining. Immunohistochemical analyses of $A\beta$ load in the hippocampi of TgSwDI mice treated with oleocanthal for 4 weeks (5 months old at the end of treatment, 5 mg/kg/day administered intraperitoneally) showed a significant reduction in total $A\beta$ levels (detected by 6E10 antibody) and in $A\beta$ plaques (detected by ThS). Semiquantitative analysis for total $A\beta$ demonstrated a significant 30% reduction in the area covered by $A\beta$ in the hippocampus of oleocanthal-treated mice compared to normal saline treated mice ($P < 0.01$; Figure 1A). Moreover, staining analysis of $A\beta$ plaques by ThS assay showed a significant reduction in the load of $A\beta$ plaques by 28% ($P < 0.01$; Figure 1B). TgSwDI mouse model is also characterized by the accumulation of $A\beta$ in the brain blood vessels, which results in the development of cerebral amyloid angiopathy (CAA). CAA is a pathological feature present concomitantly with AD at high frequency.²⁹ To test the effect of oleocanthal on the vascular deposit of $A\beta$, immunohistochemical analysis of $A\beta$ colocalization with collagen-IV (a marker of microvessels) in the hippocampus was performed. Findings revealed a significant reduction in $A\beta$ -immunoreactive microvessels in oleocanthal-treated group compared to the control group (Figure 1C) with average of $A\beta$ and collagen-IV Pearson's colocalization coefficient were significantly reduced from 0.197 (control group) to 0.046 (oleocanthal group). This data support a protective effect of oleocanthal against both CAA and AD.

To explain this reduction in $A\beta$ deposition, the effect of oleocanthal on $A\beta$ production and clearance in the brain of TgSwDI mice was evaluated. Oleocanthal effect on $A\beta$ production was assessed by monitoring levels of full length and shorter forms of amyloid precursor proteins (APP) in the mice brains. $A\beta$ is derived from sequential proteolytic

processing of APP.³⁰ Two principal APP processing pathways have been identified: the amyloidogenic pathway, which leads to $A\beta$ generation; and the nonamyloidogenic pathway, which prevents $A\beta$ generation.³¹ In the amyloidogenic pathway, the β -secretase activity initiates $A\beta$ generation by shedding a large part of the ectodomain of APP (sAPP β) generating an APP carboxy-terminal fragment (β CTF or C99), which is then cleaved by γ -secretase to liberate $A\beta$ to the brain interstitial fluid (ISF).³⁰ In the nonamyloidogenic pathway, APP is cleaved approximately in the middle of the $A\beta$ region by α -secretase.³² This processing step generates a large part of the ectodomain of APP (sAPP α) and a truncated APP CTF (α CTF or C83), which lacks the amino-terminal portion of the $A\beta$ domain.³² Therefore, increase in sAPP α or decrease in full length APP (APP-FL) or sAPP β would be associated with a reduction in brain $A\beta$ production. In this study, we measured the brain levels of APP-FL, sAPP α , and sAPP β , by Western blot, to assess the effect of oleocanthal on APP processing and $A\beta$ production. The results showed that oleocanthal treatment did not change the levels of APP-FL, sAPP α , or sAPP β (Figure 2) and, therefore, did not affect APP processing. These results suggest that reduction in hippocampal $A\beta$ load is caused by a mechanism other than $A\beta$ production.

Although production of $A\beta$ increases significantly in early onset familial AD, increasing evidence suggests that $A\beta$ accumulation in the brain of late-onset AD patients is related to its impaired clearance from the brain.³³ Moreover, mutations in $A\beta$ sequence, such as the Dutch and Iowa mutations, increase $A\beta$ propensity to aggregate specifically on microvessels and decrease its cerebral clearance in patients with familial CAA.^{28,34} Therefore, reduction in cerebral clearance of $A\beta$ is considered one of the major factors contributing to $A\beta$ accumulation and subsequent development of late-onset CAA and AD. Clearance of $A\beta$ from the brain takes place by three pathways, transport across the BBB, brain degradation, and bulk flow of cerebrospinal fluid.³⁵ Transport across the BBB significantly contributes to the total clearance of $A\beta$ and was estimated to be 62% in mice.³⁶ Given this major contribution of the BBB to $A\beta$ clearance, we next evaluated oleocanthal effect on $A\beta$ clearance across the BBB using the brain clearance index method (BCI) where ¹²⁵I- $A\beta_{40}$ was stereotaxically microinjected into the mice brains. TgSwDI mice express $A\beta$ peptides with Dutch and Iowa (DI) mutations, however, in the BCI study, wild type $A\beta_{40}$, not mutated $A\beta$, was used to evaluate the modulatory effect of oleocanthal on $A\beta$ clearance for the following reasons: the slow clearance rate of DI-mutated $A\beta$ peptides and their high propensity to aggregate in buffer solutions, which make their use in the clearance studies difficult and impractical when compared to $A\beta_{40}$. Yet, as wild type $A\beta$ and DI- $A\beta$ peptides use the same clearance proteins expressed at the BBB,³⁴ it is expected that any alteration in the expression of $A\beta$ transport proteins expressed at the BBB to modulate the clearance of both wild type and DI-mutated $A\beta$ peptides. Findings from the BCI experiments demonstrated a significant ~18% increase in total brain clearance (BCI_{total}) of ¹²⁵I- $A\beta_{40}$ from $38.4 \pm 4.2\%$ in normal saline treated mice to $56.7 \pm 5.6\%$ in oleocanthal treated mice ($p = 0.013$; Figure 3A), a value that is similar to that observed previously in young aged wild type mice.^{16,36} According to our results, this increase in total $A\beta$ clearance was in part due to the enhanced removal of $A\beta$ across the BBB where oleocanthal treatment significantly increased the BBB clearance (BCI_{BBB}) of ¹²⁵I- $A\beta_{40}$ by ~13% from $26.2 \pm 4.6\%$ in normal saline treated mice to $39.5 \pm 2.7\%$ in

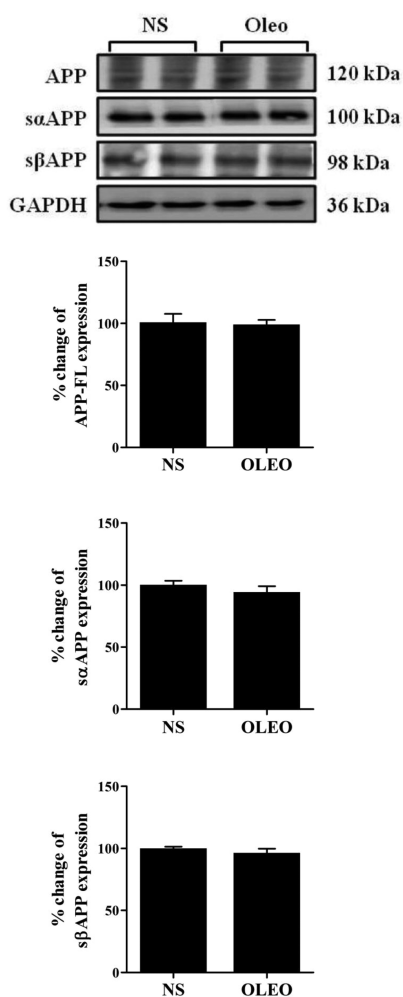


Figure 2. Effect of oleocanthal (Oleo) treatment on APP expression in brain homogenate. Representative blots and densitometry analyses of full length APP (APP-FL), sAPP α , and sAPP β showed that oleocanthal treatment for 4 weeks starting at the age of 4 months did not modulate the processing of APP as demonstrated comparable levels of full length APP, sAPP α , and sAPP β between oleocanthal and normal saline treatment groups. Data is presented as mean \pm SEM of 4–6 mice in each group (ns, not significant; * P < 0.05 and ** P < 0.01). Bands presented are from independent preparations.

oleocanthal treated mice. ($p = 0.026$; Figure 3A), which is also approaching the normal value observed in wild type mice.³⁶ This data demonstrated that oleocanthal treatment significantly enhanced $A\beta$ clearance, mainly across the BBB, thus contributing to the observed reduced $A\beta$ load in the brains of TgSwDI mice. To explain $A\beta$ enhanced clearance across the BBB, brain microvessels were isolated for analysis. $A\beta$ removal from the brain across the BBB is mainly facilitated by low density lipoprotein receptor-related protein-1 (LRP1) and P-glycoprotein (P-gp).^{37,38} Several studies including ours have demonstrated role of both proteins in $A\beta$ clearance and that their up-regulation enhances $A\beta$ peptides clearance.^{16,34,36–39} Similarly, mice treatment with oleocanthal significantly increased the expression of P-gp and LRP1 compared to the vehicle treated group (Figure 3B) as determined by Western blot. Densitometry analyses of the bands showed a significant increase by $\sim 25\%$ in P-gp and $\sim 27\%$ in LRP1 expressions in the brain capillaries of oleocanthal group (Figure 3B). In addition to transport proteins, and consistent with our previous

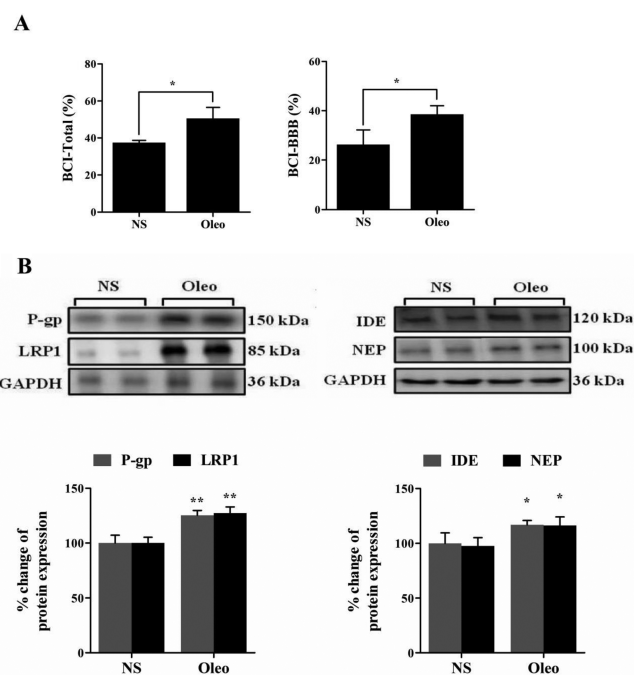


Figure 3. In vivo clearance of ¹²⁵I- $A\beta$ ₄₀ from brain of TgSwDI mice. (A) Enhanced total brain clearance (BCI-total (%)) and BBB clearance (BCI-BBB (%)) of ¹²⁵I- $A\beta$ ₄₀ was observed after oleocanthal treatment for 4 weeks. (B) Representative blots and densitometry analysis of P-gp and LRP1 expressions in mice brains' microvessels, and $A\beta$ degrading enzymes IDE and NEP in mice brains' homogenates. Data is presented as mean \pm SEM of 4–6 mice in each group (* P < 0.05 and ** P < 0.01). Western blot bands presented are from independent preparations.

findings in wild type mice,¹⁶ oleocanthal treatment significantly increased the expression of $A\beta$ degrading enzymes NEP and IDE in mice brains' homogenates (Figure 3B). These findings are significant because they emphasize the beneficial effect of oleocanthal to reduce brain levels of not only wild type $A\beta$ peptides but to include Dutch- and Iowa-mutated $A\beta$, found in familial cases, that have been recognized for their slow brain clearance,^{28,34} therefore extending its effect to, beside the sporadic type, to familial AD.

ApoE-dependent $A\beta$ clearance is another well-established pathway known for its high efficiency in cerebral $A\beta$ removal.^{40,41} This pathway includes ApoE and ABCA1 that are transcriptionally regulated by the nuclear receptors peroxisome proliferator-activated receptor gamma (PPAR γ) and liver X receptors (LXRs).⁴² The mechanism by which ApoE-mediated pathway enhances $A\beta$ clearance could be via enhancing $A\beta$ phagocytosis by macrophages and microglial cells and/or other clearance pathways.^{43,44} To evaluate the effect of oleocanthal on this pathway, Western blot analysis for ABCA1, ApoE, PPAR γ and LXR was performed in brains' homogenates. Oleocanthal was able to increase the expression of ABCA1, ApoE, and PPAR γ but not LXR. Densitometry analysis showed a significant $\sim 20\%$ increase in ABCA1 expression (P < 0.01; Figure 4A), and a moderate but significant $\sim 12\%$ increase in ApoE levels (P < 0.05; Figure 4B). This increase in the expression of ABCA1 and ApoE, was associated with increased expression of PPAR γ ($\sim 26\%$, Figure 4C; P < 0.01) but not LXR (Figure 4D). PPAR γ and LXR act in a feed-forward manner to induce the expression of ABCA1 and ApoE.⁴² The significance of inducing this pathway was previously reported in

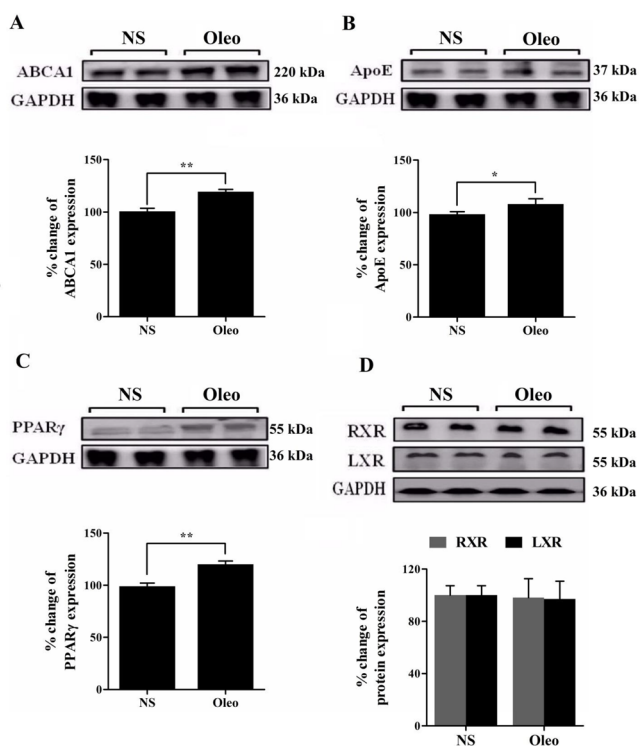


Figure 4. Oleocanthal (Oleo) treatment enhanced ApoE-dependent clearance pathway of $A\beta$ through the activation of PPAR γ expression. Representative blots and densitometry analysis of ABCA1 (A) and ApoE (B) showed significant up-regulation in their expressions in the brain tissue of TgSwDI mice after oleocanthal (Oleo) treatment. (D) Representative blot and densitometry analysis show significant induction in the expression of PPAR γ in oleocanthal treated mice. (D) Expression of LXR and RXR were not affected by oleocanthal treatment. Data is presented as mean \pm SEM of 4–6 mice in each group (* P < 0.05). Western blot bands presented are from independent preparations.

several studies; for example, Zolezzi et al. reported that activation of PPAR γ reduces $A\beta$ levels and improves cognitive function in mouse models of AD,⁴³ and Cramer et al., who reported that enhanced expression of PPAR γ to stimulate ApoE and ABCA1 expression and thus $A\beta$ clearance.⁴⁴ Interestingly, PPAR γ has also shown to regulate LRP1 and P-gp expressions.^{45,46} In vivo and in vitro studies demonstrated treatment with the PPAR γ activators cilostazol, a selective phosphodiesterase 3 inhibitor, and *Thunbergia laurifolia*, widely used as an antidote, to upregulate hepatic LRP1 protein expression in vivo⁴⁵ and P-gp activity in vitro,⁴⁶ respectively. Thus, enhanced LRP1 and P-gp efflux function by oleocanthal could also be mediated, at least in part, by activating PPAR γ . The effect of oleocanthal on modulating expression of the nuclear receptor retinoid-X receptor (RXR), that forms obligate heterodimers with PPAR γ and LXR,⁴⁷ was also assessed by Western blot, however findings demonstrated oleocanthal does not alter RXR expression (Figure 4D). Collectively, these findings provide an additional mechanism by which oleocanthal decreases levels of $A\beta$ in the brains of TgSwDI mice by enhancing $A\beta$ clearance across the BBB and ApoE-dependent pathway.

Besides $A\beta$ pathology, in the current work, we investigated the effect of oleocanthal treatment on tau expression and phosphorylation in the brains of TgSwDI mice by Western blot. Antibodies against total tau and different phosphorylation sites

of tau, including serine-214, serine-262, threonine-212, and threonine-231 were used. Tau is a microtubule-associated protein that accumulates in an abnormally hyper-phosphorylated state forming intracellular filamentous deposits in AD.⁴⁸ Tau promotes the assembly of tubulin into microtubules and stabilizes the microtubule structure that supports axoplasmic transport.⁴⁸ In AD, hyper-phosphorylation of tau at serine and threonine residues such as serine-214, serine-262, threonine-212, and threonine-231 inhibits significantly the binding of tau to microtubules and making tau more cytotoxic.^{48,49} In contrast to $A\beta$ pathology, our results showed comparable expression level and phosphorylation in all studied epitopes between oleocanthal and normal saline treated groups (Figure 5). This

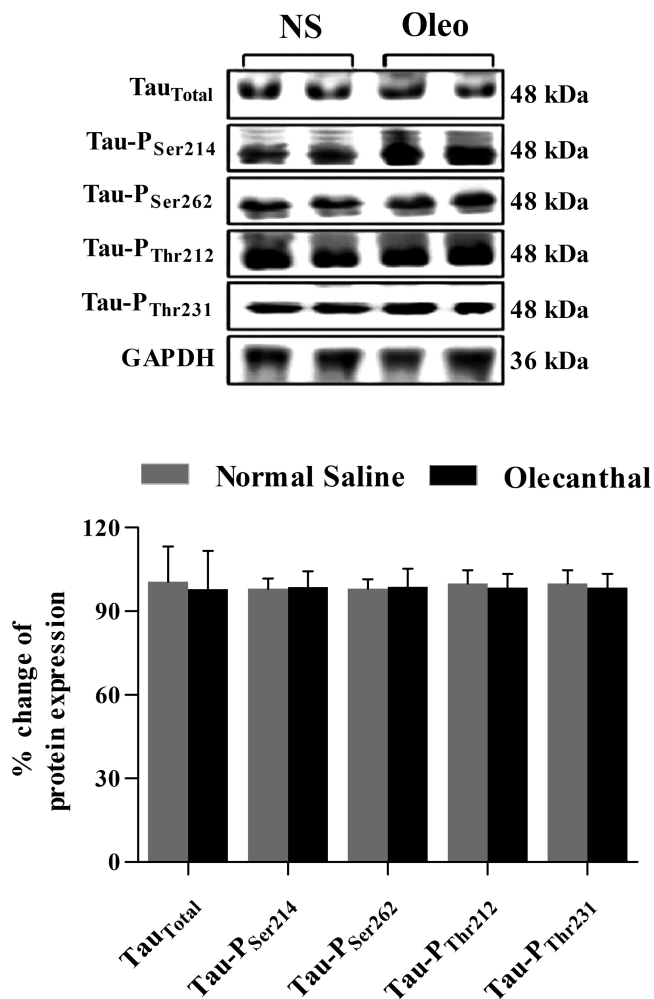


Figure 5. Treatment of TgSwDI mice with oleocanthal did not affect the expression or phosphorylation of tau protein as shown in the representative blots and their densitometry total-tau and phosphorylated tau at serine-214, serine-262, threonine-212, and threonine-231 residues in the brain homogenates of TgSwDI mice. Data is presented as mean \pm SEM of 4–6 mice in each group.

lack of oleocanthal effect against tau could be related to the limited treatment time (4 weeks). Previous studies demonstrated a hierarchical relationship between $A\beta$ and tau pathologies, with $A\beta$ causing tau to accumulate and to undergo phosphorylation.⁵⁰ Therefore, it is conceivable that longer administration time of oleocanthal could alter tau pathogenesis because of reduction in $A\beta$ load.

The anti-inflammatory effect of oleocanthal in mice brains was also evaluated. Dysfunctional astrocytes have been recognized as an additional pathological alteration observed in AD. Astrocytes are essential in the control of brain homeostasis and support neurons to function. Astrocytes contribute to synaptogenesis and dynamically modulate information processing and signal transmission, regulate neural and synaptic plasticity, and provide trophic and metabolic support to neurons as well as the BBB.⁵¹ Available evidence showed that A β deposition could modify astrocytes physiological function and acquire a reactive phenotype.⁵² Activation of astrocytes is basically a protective response to remove unwanted stimuli. However, when this activation is prolonged, astrocytes will have damaging effects where they could foster neuroinflammatory response and secret different cytokines and proinflammatory mediators that are neurotoxic.^{53,54} Reducing astrocytes activation has been suggested as an additional therapeutic approach to restore supportive astrocytes functions and prevent further inflammatory mediated cell death by A β and oxidative stress.⁵⁵ While the anti-inflammatory effect of oleocanthal has been reported previously,¹⁵ its anti-inflammatory effect on astrocytes activation caused by A β and on brain levels of cytokines is not yet known. One of the earliest markers of astrocyte inflammatory activation is the increased levels of glial fibrillary acidic protein (GFAP), and the long shape with thick branches. GFAP is rapidly induced by different inflammatory mediators and brain stressful events including A β deposits.⁵⁶ Our results demonstrated the ability of oleocanthal to reduce astrocytes activation (Figure 6A, B) and attenuate GFAP intensity by \sim 41% ($P < 0.01$, Figure 6B).

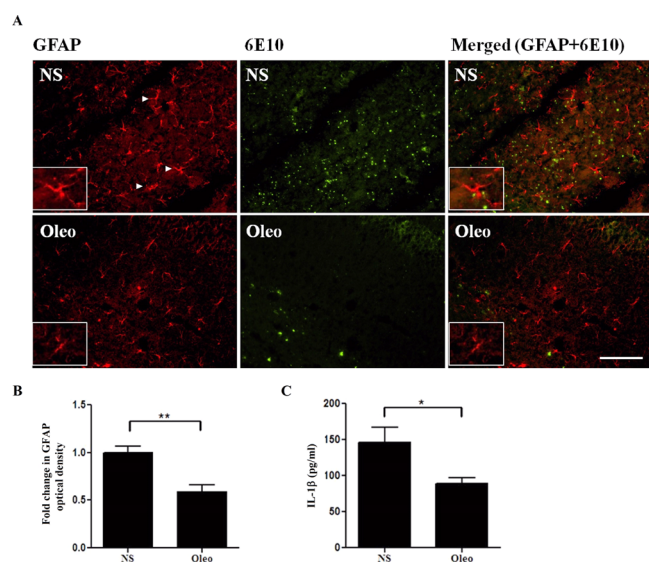


Figure 6. Oleocanthal (Oleo) treatment reduces astrocytes activation in the hippocampus of TgSwDI and brain IL-1 β . (A) Representative hippocampus sections double-stained with GFAP antibody and anti-A β 6E10 to detect activated astrocytes and A β load, respectively. Arrows in normal saline group (NS) indicate activated astrocytes with long and thick branches (seen at higher magnification in the closed inserts). (B) Quantitative analysis of GFAP optical density showed a significant reduction in astrocytes activation associated with reduced A β levels. Data is presented as mean \pm SEM of 4–6 mice in each group. Scale bar, 50 μ m. (C) Oleo treatment reduced brain levels of IL-1 β ($n = 4$ /group). (* $P < 0.05$ and ** $P < 0.01$). TgSwDI mice were treated with oleocanthal (5 mg/kg/day) or NS for 4 weeks beginning at age 4 months.

In addition, this reduced activation ameliorated the astrocytes shape when compared to the control group (Figure 6A). This reduction in astrocytes activation could be attributed to the reduced levels of A β (Figure 1). Moreover, the anti-inflammatory response of oleocanthal was further supported by the significant reduction in brains' levels of the cytokine interleukin-1 β (IL-1 β) by \sim 39% ($P < 0.05$, Figure 6C). This anti-inflammatory effect of oleocanthal is consistent with that of a previously reported in vitro effect on IL-1 β levels in murine chondrocyte cells.⁵⁷

Next, to evaluate whether the observed effect of oleocanthal on A β clearance in the brains of AD mouse model could be extended to humans, a series of in vitro experiments with hCMEC/D3 and SH-SY5Y-APP cells were performed (Figure 7A). hCMEC/D3 cells were used as a representative model of human BBB endothelial cells, and SH-SY5Y-APP cells as a model for human neuronal cells which secret A β . Transport studies showed that treatment of cultured cells with 0, 1, 5, and 10 μ M oleocanthal caused a concentration-dependent increase, up to 50%, in the basolateral to apical transport of A β (TQ $_{B \rightarrow A}$) secreted from SH-SY5Y-APP cells (Figure 7B). This increase was associated with a concentration dependent increase in P-gp and LRP1 expression in hCMEC/D3 cells after 72 h treatment (Figure 7C), which is consistent with the above in vivo results and our previous study.¹⁶ In addition, oleocanthal effect on the production and secretion of A β from SH-SY5Y-APP cells was evaluated by measuring A β_{40} , A β_{42} and the different forms of APP levels by Western blot. As shown in Figure 7D, the expression of A β_{40} and A β_{42} peptides secreted in the media of SH-SY5Y-APP cells, separately treated with oleocanthal for 72 h, were comparable to those without treatment ($P > 0.05$). Similarly, oleocanthal treatment did not modulate the levels of sAPP α and sAPP β (Figure 7E), confirming that oleocanthal has no effect on the production and secretion of A β from SH-SY5Y-APP. In addition, these constant and comparable levels of A β peptides as well as sAPP forms suggest that oleocanthal has no γ -secretase modulatory properties. Together, these findings suggest that the positive effect of oleocanthal could be extended to humans, and that oleocanthal is a promising therapeutic molecule against AD.

Collectively, findings from this study showed that oleocanthal treatment has significantly reduced the total A β levels in TgSwDI brains hippocampi and decreased A β deposits on brain microvessels. The reduction in A β levels could be explained, at least in part, to the enhanced A β clearance across the BBB via the up-regulation of P-gp and LRP1, and up-regulation of the ApoE-dependent pathway. In addition, oleocanthal demonstrated an anti-inflammatory effect where it reduced astrocytes activation and IL-1 β brain levels. To account for species differences, we were able to recapitulate the protective effect of oleocanthal against amyloid pathology in a human-based in vitro model. Therefore, oleocanthal could have effect on human similar to that observed in transgenic mice. These effects were statistically significant, suggesting oleocanthal treatment for longer, and possibly at earlier time, that is, before A β brain accumulation starts, could be therapeutically beneficial for AD and CAA prevention and/or treatment. In conclusion, oleocanthal is a novel natural molecule possesses several beneficial effects via targeting multiple pathological aspects of AD, and holds a promise for development as a potentially effective AD drug. Studies investigating oleocanthal systemic availability and dosage requirements for translational application are currently in progress.

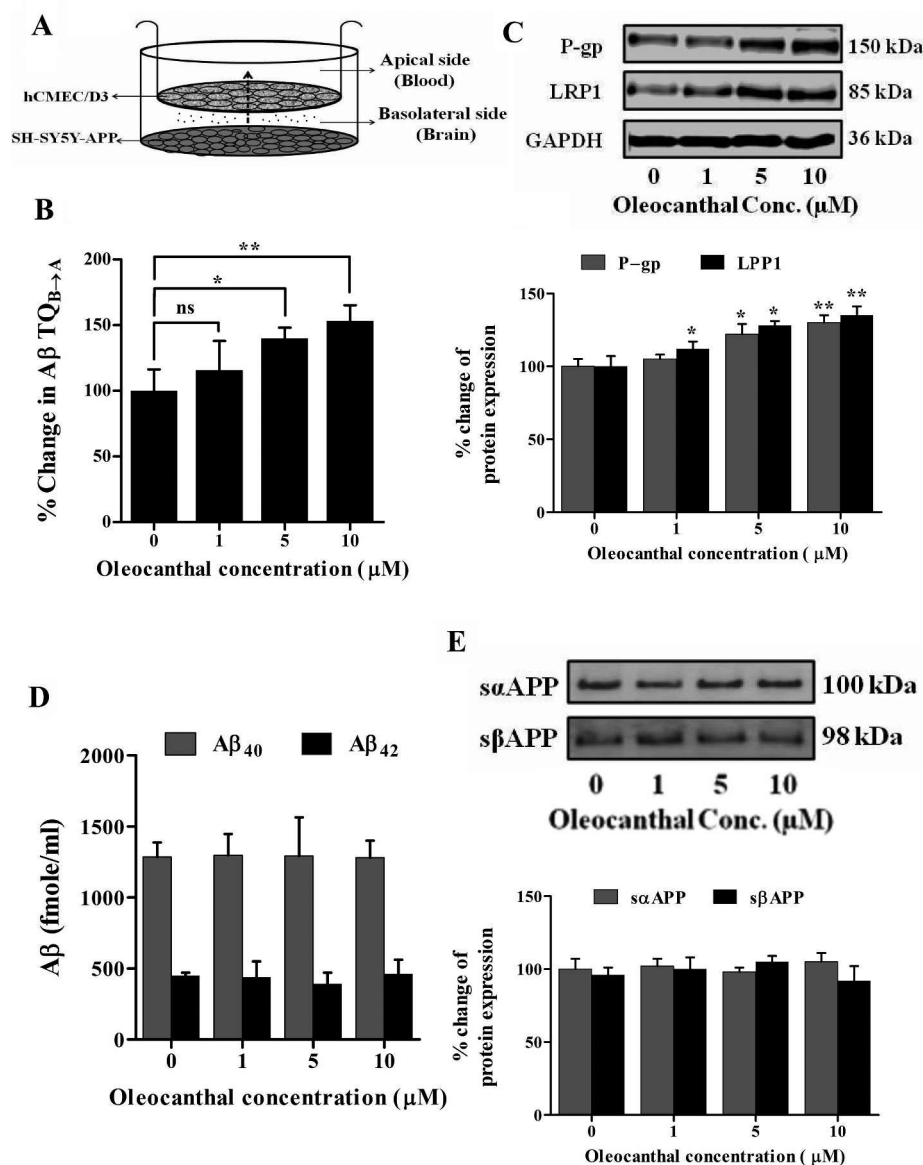


Figure 7. Oleocanthal (Oleo) enhances $A\beta$ transport across brain endothelial monolayer in an in vitro model of neurovascular unit. (A) Schematic presentation for in vitro model of the neurovascular unit that has been used to assess the effect of oleocanthal on $A\beta$ transport across brain endothelium. (B) Effect of increasing concentration of oleocanthal on the transport of $A\beta$ secreted from SH-SY5Y-APP cells across hCMEC/D3 monolayer. $A\beta$ transport is determined as transport quotient ($A\beta$ -TQ_{B→A}). (C) Effect of increasing concentration of oleocanthal on the expression of P-gp and LRP1 in hCMEC/D3 cells as measured by Western blot. Densitometry analysis shows a concentration dependent increase in P-gp and LRP1 after treatment with oleocanthal. (D) ELISA quantitative analysis of the levels of human $A\beta_{40}$ and $A\beta_{42}$ in the media of SH-SY5Y-APP cells separately treated with increasing concentrations of oleocanthal shows that oleocanthal has no effect on $A\beta$ production and secretion. (E) Effect of increasing concentration of oleocanthal on APP processing. Representative blots and densitometry analysis of sAPP α and sAPP β in the media of SH-SY5Y-APP cells confirmed that oleocanthal has no effect on APP processing. Data is presented as mean \pm SEM of three independent experiments (ns, not significant; * P < 0.05 and ** P < 0.01).

METHODS

Oleocanthal Extraction. Oleocanthal was extracted as previously reported.⁵⁸ Extra-virgin olive oil (EVOO; Member's Mark, batch no. VF1-US102808, Italy) was used as a source for extracting oleocanthal. Oleocanthal was first eluted from lipophilic Sephadex LH20 packed column (bead size 25–100 μ m, Sigma-Aldrich, MO) with *n*-hexane:CH₂Cl₂ (1:9) system. Next, oleocanthal was purified from its rich fraction on C-18 reversed phase Bakerbond octadecyl packed column (bead size 40 μ m; Mallinckrodt Baker) using isocratic CH₃CN:H₂O (40:60). A purity of >90% was established for oleocanthal as assessed by TLC, ¹H NMR spectroscopy, and HPLC analysis.

Animals Treatment. TgSwDI mice were housed in plastic cages under standard conditions, 12 h light/dark cycle, 22 °C, 35% relative humidity, and ad libitum access to water and food. The TgSwDI mice express human APP under control of Thy 1.2 neuronal promoter harboring double Swedish mutations and the Dutch and Iowa vasculotropic $A\beta$ mutations.²⁸ Two groups were assigned to test the effect of oleocanthal treatment, one group received daily intraperitoneal injection with 5 mg/kg oleocanthal (Oleo group, n = 6 mice) dissolved in normal saline containing 5% DMSO and the second group received daily intraperitoneal injection of normal saline containing 5% DMSO (NS group, n = 6 mice). To minimize confounding, all experiments were performed using male age-matched mice. Oleocanthal and normal saline treatments were initiated at age of

4 months and continued for 4 weeks. The Institutional Animal Care and Use Committee of the University of Louisiana at Monroe approved all procedures with National Institutes of Health guidelines.

Immunohistochemical Analyses. For detection of total A β load, formaldehyde-fixed cryostat brain slices were immunostained with 6E10 human-specific anti-A β antibody (Biolegend, CA) at 1:200 dilution followed by fluorescein-conjugated donkey anti-mouse IgG (Santa Cruz, TX). For detection of A β -plaque load in hippocampus, the brain tissue sections were stained with a filtered 1% Thioflavin-S (ThS; Sigma-Aldrich, MO) solution in 80% ethanol for 15 min, as described previously.⁵⁹ Double immunostaining of astrocytes with A β and capillaries with A β was performed using rabbit polyclonal GFAP antibody (Santa Cruz) at 1:200 dilution for astrocytes detection, rabbit polyclonal collagen IV antibody (Millipore, CA) at 1:200 dilution for capillaries detection and Alexa Fluor 488 conjugated anti-A β antibody (6E10) for A β detection followed by IgG-CFL 594 conjugated donkey antirabbit (Santa Cruz) as a secondary antibody for astrocytes and capillaries detection. Images were captured using Nikon Eclipse Ti-S inverted fluorescence microscope (Norcross, GA) at a total magnification of 40 \times for A β plaque load detection, and 200 \times for astrocytes/A β and capillaries/A β double immunostaining. For each treatment, images acquisition was performed in 6 groups of tissue sections spanning the hippocampus, each separated by 150 μ m and each containing three 15 μ m sections (total of 18 sections per mouse). Quantification of total A β load, A β -plaque load and GFAP optical density in the hippocampus was performed using ImageJ version 1.44 software after adjusting for threshold (Research Services Branch, NIMH/NIH, Bethesda, MD). Total A β load in the hippocampus was measured as a percentage of A β -covered area and A β -plaque load was expressed as the total number of A β -plaque. Pearson's correlation coefficient was calculated to describe the colocalization correlation between A β and collagen-IV as previously described⁶⁰ using ImageJ.

Brain Clearance of ¹²⁵I-A β ₄₀. In vivo A β ₄₀ clearance was investigated using the BCI method as described previously.³⁶ Animals were anesthetized followed by the insertion of a stainless steel guide cannula into the right caudate nucleus of mice brains. A tracer fluid (0.5 μ L) containing ¹²⁵I-A β ₄₀ (30 nM, PerkinElmer, MA) and ¹⁴C-inulin (0.02 mCi, American Radiolabeled Chemicals, MO) prepared in extracellular fluid buffer (ECF) was microinjected. Thirty minutes later, brains were rapidly collected. One hemisphere of the brain was used for ¹²⁵I-A β ₄₀ analysis and the second hemisphere was used for microvessels isolation as described below. Calculations of ¹²⁵I-A β ₄₀ clearance were performed as described previously.³⁶ Using trichloroacetic acid (TCA) precipitation intact (precipitate) and degraded (supernatant) ¹²⁵I-A β ₄₀ were determined in brain tissue using a Wallac 1470 Wizard Gamma Counter (PerkinElmer, MA). ¹⁴C-inulin in the precipitate and supernatant were also determined using a Wallac 1414 WinSpectral Counter (PerkinElmer). The ¹²⁵I-A β ₄₀ brain clearance index (BCI_{total}(%)) and clearance of ¹²⁵I-A β ₄₀ across BBB (BCI_{BBB}(%)) were determined as described previously.³⁶

Brain Microvessel Isolation. Brain microvessels were isolated as described previously.⁵⁵ Each brain hemisphere was homogenized in ice-cold DPBS followed by the addition of one volume of 30% Ficoll 400 (Sigma-Aldrich). Homogenates were centrifuged at 8000g for 10 min, and the resulting pellets were suspended in ice-cold DPBS containing 1% BSA and passed over a glass bead column to collect microvessels adhering to the glass beads. Isolated microvessels were used for determine P-gp and LRP1 expression by Western blot.

IL-1 β ELISA. For detection of IL-1 β levels in brain homogenate, anti-mouse IL-1 beta Quantikine ELISA kit (R&D Systems, MN) was used according to the manufacturer's instructions. IL-1 β concentrations (in pg/mL) were calculated from standard curves. All samples were run at least in triplicate.

Cell Culture. Human brain endothelial cells (hCMEC/D3; kindly provided by Dr. P. O. Couraud, Institute Cochin, Paris, France), passage 25–35, were used as a representative model for human BBB. hCMEC/D3 cells were cultured in EBM-2 medium (Lonza, MD) supplemented with 1 ng/mL human basic fibroblast growth factor (Sigma-Aldrich), 10 mM HEPES, 1% chemically defined lipid concentrate (Gibco, NY), 5 μ g/mL ascorbic acid, 1.4 μ M hydro-

cortisone, 1% penicillin–streptomycin, and 5% of heat-inactivated FBS gold (GE Healthcare Life Sciences, PA). Human neuroblastoma cells (SH-SY5Y) stably expressing wild-type human APP695 (kindly provided by Dr. Elizabeth A. Eckman, Biomedical Research Institute of New Jersey, NJ) were maintained in DMEM supplemented with 10% FBS, glutamine, penicillin (100 units/mL) and streptomycin (100 μ g/mL), and the selective antibiotic Geneticin at 400 μ g/mL (Gibco).⁶¹ Cultures were maintained in a humidified atmosphere (5%CO₂/95% air) at 37 °C and media was changed every other day.

Effect of Oleocanthal on A β Transport across hCMEC/D3 Monolayer. The transport of A β and ¹⁴C-inulin, as a marker for paracellular diffusion, was measured across hCMEC/D3 monolayer after treatment with different oleocanthal concentrations. To prepare hCMEC/D3 cell monolayers, transwell polyester membrane inserts, 6.5 mm diameter with 0.4 μ m pores (Corning, NY), were coated with rat tail collagen-IV (150 μ g/mL) for 90 min at 37 °C. Cells were plated onto coated inserts at a seeding density of 50 000 cells/cm²; medium was changed every other day. Transepithelial electrical resistance (TEER) was measured using an EVOM epithelial volt-ohmmeter with STX2 electrodes (World Precision Instruments, FL). hCMEC/D3 cell monolayers were used for A β transport experiments on day 6 of culture. On day 6, the TEER value was measured and ranged from 35 to 40 $\Omega \times$ cm², consistent with previously reported values for this cell line. Cells were treated for 72 h starting from third day of seeding with increasing concentration of oleocanthal (0, 1, 5, and 10 μ M) added to the apical side of the model (Figure 7A). At the end of treatment, transwells were transferred to 24-well plate that contains APP695-transfected SH-SY5Y cells at 70–80% confluency. Basolateral to apical (B \rightarrow A) transport studies of A β secreted from SH-SY5Y-APP transfected cells were initiated by addition of 800 μ L of fresh prewarmed media that contains 0.05 mM ¹⁴C-inulin to basolateral chamber and 200 μ L of fresh media was added to the apical chambers. Cells were maintained in a humidified atmosphere (5%CO₂/95% air) at 37 °C for the time course of the transport experiments (up to 12 h). At the end of incubation period (12 h), media from both chambers were separately collected for A β analysis and ¹⁴C-inulin measurements. A β concentrations in basolateral and apical chambers were measured using a highly specific sandwich ELISA. Rabbit anti-A β 40 (Millipore, CA, Cat# AB5737) and rabbit anti-A β 42 (Calbiochem, CA, Cat# PC150) monoclonal antibodies specific against the C-termini of human A β 40 and A β 42, respectively, were used as capturing antibodies. Antibodies were coated at 5 μ g/ml (100 ng/well) on a Maxisorp ELISA plate (Thermo Scientific, IL) to capture A β . Detection was achieved with HRP-conjugated 6E10 (Covance Research Products, MA) monoclonal antibody specific against N-terminus of human A β (aa. 3-8 human A β sequence) at 1 μ g/ml. For ¹⁴C-inulin measurements, samples were mixed with 5 mL of scintillation cocktail then dpm was measured using a Wallac 1414 Liquid Scintillation Counter. Amount of A β and ¹⁴C-inulin in basolateral and apical chambers were calculated as ng and dpm, respectively. The transport quotients of B \rightarrow A (A β -TQ_{B \rightarrow A}) transport were calculated as described previously.³⁶

To study the effect of oleocanthal on A β transporters/receptors expression in hCMEC/D3 cells, Western blot analysis was used to measure the expression of P-gp and LRP1 after treatment of hCMEC/D3 cells with oleocanthal. hCMEC/D3 cells were seeded in 100 mm cell culture dishes (Corning) at a density of 1 \times 10⁶ cells per dish. The cells were allowed to grow to 70% confluency before treatment with different concentrations of oleocanthal in a humidified atmosphere (5% CO₂/95% air) at 37 °C. Cells were treated for 72 h with control media or oleocanthal (0, 1, 5, and 10 μ M). At the end of treatment period, cells were washed with ice cold PBS, scraped, and centrifuged at 500 rpm for 10 min, and then the pellet was dissolved in 100 μ L of RIPA buffer containing complete mammalian protease inhibitor mixture (Sigma-Aldrich).

Effect of Oleocanthal on A β Production by SH-SY5Y-APP Transfected Cells. To study the effect of oleocanthal on the production of A β , SH-SY5Y-APP cells were seeded in 24-well plates and maintained as described above. At 30–40% confluency, SH-SY5Y-APP cells were treated with oleocanthal at 0, 1, 5, and 10 μ M for 72 h.

At the end of the treatment period, media containing oleocanthal was removed, cells were washed with prewarmed media, and then fresh prewarmed 300 μ L media was added to the cells. After 12 h, media was collected for $A\beta$ and sAPP analyses. $A\beta_{40}$ and $A\beta_{42}$ levels in medium were measured by ELISA. The levels of sAPP α and sAPP β in the medium from cultured SH-SY5Y-APP cells were determined by Western blot analysis.

Western Blot Analysis. Protein extracts were prepared from cell lysates, brain microvessels, or brain tissues with RIPA buffer containing 1 \times complete mammalian protease inhibitor mixture followed by centrifugation at 21 000g for 1 h at 4 $^{\circ}$ C. The supernatant was collected as protein extract and stored at -80° C until the time of analysis. Protein concentrations were determined by the BCA method. For Western blot analysis, 25 μ g of protein was resolved on 8% bis-tris gels in 3-(*N*-morpholino)propanesulfonic acid buffer system and electrotransferred onto a 0.45 μ m nitrocellulose membrane. Membranes were blocked with 2% BSA and incubated overnight with monoclonal antibodies for P-gp (C-219; Covance Research Products), LRP1 (Calbiochem), ABCA1, ApoE, LXR, RXR, PPAR γ , or GAPDH (Santa Cruz). Specific antibodies against sAPP α and sAPP β were obtained from Immuno-Biological laboratories (IBL). Total tau protein was detected by a phosphate-independent antitau monoclonal antibody (clone Tau-5; Thermo Scientific). Specific antibodies recognizing tau protein phosphorylated at serine residues 214 and 262 and at threonine residues 212 and 231 were used (Signalway). For detection, the membranes were washed free of primary antibody and incubated with HRP-labeled secondary IgG antimouse antibody for P-gp, ABCA1, sAPP α , tau Ab-2, and GAPDH (Santa Cruz); anti-rabbit antibody for LRP1, LXR, RXR, PPAR γ , and phosphorylated tau (Santa Cruz); and anti-goat antibody for ApoE (Santa Cruz). The bands were visualized using a Pierce chemiluminescence detection kit (Thermo Scientific). Quantitative analysis of the immunoreactive bands was performed using Li-Core luminescent image analyzer (LI-COR Biotechnology), and band intensity was measured by densitometric analysis. Three independent Western blotting experiments were carried out for each treatment group.

Statistical Analysis. Unless otherwise indicated, the data were expressed as mean \pm SEM. The experimental results were statistically analyzed for significant difference using two-tailed Student's *t* test for two groups. Values of *P* < 0.05 were considered statistically significant.

AUTHOR INFORMATION

Corresponding Author

*E-mail: kaddoumi@monroe.lsu.edu. Mailing address: Department of Basic Pharmaceutical Sciences, School of Pharmacy, University of Louisiana at Monroe, 1800 Bienville Dr., Monroe, LA 71201.

Author Contributions

[§]H.Q. and Y.S.B.: Equal contribution.

Funding

This project was supported by a grant from the National Institute of General Medical Sciences (P20GM103424) from the National Institutes of Health.

Notes

The authors declare no competing financial interest.

ACKNOWLEDGMENTS

We thank Dr. P. O. Couraud, Institute Cochin, Paris, France for providing the hCMC/D3 cell line. We thank Dr. Elizabeth A. Eckman, Biomedical Research Institute of New Jersey, NJ, for providing the APP transfected SH-SY5Y cell line.

ABBREVIATIONS

AD, Alzheimer's disease; $A\beta$, amyloid- β ; APP, amyloid- β precursor protein; BBB, blood-brain barrier; EVOO, extra-virgin olive oil; IDE, insulin degrading enzyme; LRP1, low density lipoprotein receptor-related protein-1; NEP, neprilysin;

Oleo, oleocanthal; P-gp, P-glycoprotein; RAGE, receptor for advanced glycation end products; SDS, sodium dodecylphosphate; TCA, trichloroacetic acid; ThS, thioflavin-S

REFERENCES

- (1) Salvini, S., Sera, F., Caruso, D., Giovannelli, L., Visioli, F., Saieva, C., Masala, G., Ceroti, M., Giovacchini, V., Pitozzi, V., Galli, C., Romani, A., Mulinacci, N., Bortolomeazzi, R., Dolara, P., and Palli, D. (2006) Daily consumption of a high-phenol extra-virgin olive oil reduces oxidative DNA damage in postmenopausal women. *Br. J. Nutr.* 95, 742–751.
- (2) Filik, L., and Ozyilkan, O. (2003) Olive-oil consumption and cancer risk. *Eur. J. Clin. Nutr.* 57, 191.
- (3) Scarmeas, N., Stern, Y., Mayeux, R., and Luchsinger, J. A. (2006) Mediterranean diet, Alzheimer disease, and vascular mediation. *Arch. Neurol.* 63, 1709–1717.
- (4) Valls-Pedret, C., Sala-Vila, A., Serra-Mir, M., Corella, D., de la Torre, R., Martinez-Gonzalez, M. A., Martinez-Lapiscina, E. H., Fito, M., Perez-Heras, A., Salas-Salvado, J., Estruch, R., and Ros, E. (2015) Mediterranean Diet and Age-Related Cognitive Decline: A Randomized Clinical Trial. *JAMA Intern Med.* 175, 1094.
- (5) Tuck, K. L., and Hayball, P. J. (2002) Major phenolic compounds in olive oil: metabolism and health effects. *J. Nutr. Biochem.* 13, 636–644.
- (6) Shubair, M. M., McColl, R. S., and Hanning, R. M. (2005) Mediterranean dietary components and body mass index in adults: the peel nutrition and heart health survey. *Chronic Dis. Can.* 26, 43–51.
- (7) Corona, G., Spencer, J. P., and Dessi, M. A. (2009) Extra virgin olive oil phenolics: absorption, metabolism, and biological activities in the GI tract. *Toxicol. Ind. Health* 25, 285–293.
- (8) Scarmeas, N., Stern, Y., Mayeux, R., Manly, J. J., Schupf, N., and Luchsinger, J. A. (2009) Mediterranean diet and mild cognitive impairment. *Arch. Neurol.* 66, 216–225.
- (9) Scarmeas, N., Stern, Y., Tang, M. X., Mayeux, R., and Luchsinger, J. A. (2006) Mediterranean diet and risk for Alzheimer's disease. *Ann. Neurol.* 59, 912–921.
- (10) Tripoli, E., Giammanco, M., Tabacchi, G., Di Majo, D., Giammanco, S., and La Guardia, M. (2005) The phenolic compounds of olive oil: structure, biological activity and beneficial effects on human health. *Nutr. Res. Rev.* 18, 98–112.
- (11) Aguilera, C. M., Mesa, M. D., Ramirez-Tortosa, M. C., Nestares, M. T., Ros, E., and Gil, A. (2004) Sunflower oil does not protect against LDL oxidation as virgin olive oil does in patients with peripheral vascular disease. *Clin. Nutr.* 23, 673–681.
- (12) Cicerale, S., Lucas, L., and Keast, R. (2010) Biological activities of phenolic compounds present in virgin olive oil. *Int. J. Mol. Sci.* 11, 458–479.
- (13) Lopez, S., Bermudez, B., Montserrat-de la Paz, S., Jaramillo, S., Varela, L. M., Ortega-Gomez, A., Abia, R., and Muriana, F. J. (2014) Membrane composition and dynamics: a target of bioactive virgin olive oil constituents. *Biochim. Biophys. Acta, Biomembr.* 1838, 1638–1656.
- (14) Vissers, M. N., Zock, P. L., and Katan, M. B. (2004) Bioavailability and antioxidant effects of olive oil phenols in humans: a review. *Eur. J. Clin. Nutr.* 58, 955–965.
- (15) Beauchamp, G. K., Keast, R. S., Morel, D., Lin, J., Pika, J., Han, Q., Lee, C. H., Smith, A. B., and Breslin, P. A. (2005) Phytochemistry: ibuprofen-like activity in extra-virgin olive oil. *Nature* 437, 45–46.
- (16) Abuznait, A. H., Qosa, H., Busnena, B. A., El Sayed, K. A., and Kaddoumi, A. (2013) Olive-oil-derived oleocanthal enhances beta-amyloid clearance as a potential neuroprotective mechanism against Alzheimer's disease: in vitro and in vivo studies. *ACS Chem. Neurosci.* 4, 973–982.
- (17) Farr, S. A., Price, T. O., Dominguez, L. J., Motisi, A., Saiano, F., Niehoff, M. L., Morley, J. E., Banks, W. A., Ercal, N., and Barbagallo, M. (2012) Extra virgin olive oil improves learning and memory in SAMP8 mice. *J. Alzheimer's Dis* 28, 81–92.
- (18) Grossi, C., Rigacci, S., Ambrosini, S., Ed Dami, T., Luccarini, I., Traini, C., Failli, P., Berti, A., Casamenti, F., and Stefani, M. (2013)

The polyphenol oleuropein aglycone protects TgCRND8 mice against A β plaque pathology. *PLoS One* 8, e71702.

(19) Luccarini, I., Ed Dami, T., Grossi, C., Rigacci, S., Stefani, M., and Casamenti, F. (2014) Oleuropein aglycone counteracts A β 42 toxicity in the rat brain. *Neurosci. Lett.* 558, 67–72.

(20) Pitozzi, V., Jacomelli, M., Zaid, M., Luceri, C., Bigagli, E., Lodovici, M., Ghelardini, C., Vivoli, E., Norcini, M., Gianfriddo, M., Esposito, S., Servili, M., Morozzi, G., Baldi, E., Bucherelli, C., Dolara, P., and Giovannelli, L. (2010) Effects of dietary extra-virgin olive oil on behaviour and brain biochemical parameters in ageing rats. *Br. J. Nutr.* 103, 1674–1683.

(21) Monti, M. C., Margarucci, L., Tosco, A., Riccio, R., and Casapullo, A. (2011) New insights on the interaction mechanism between tau protein and oleocanthal, an extra-virgin olive-oil bioactive component. *Food Funct.* 2, 423–428.

(22) Pitt, J., Roth, W., Lacor, P., Smith, A. B., 3rd, Blankenship, M., Velasco, P., De Felice, F., Breslin, P., and Klein, W. L. (2009) Alzheimer's-associated A β oligomers show altered structure, immunoreactivity and synaptotoxicity with low doses of oleocanthal. *Toxicol. Appl. Pharmacol.* 240, 189–197.

(23) Selkoe, D. J. (2001) Alzheimer's disease: genes, proteins, and therapy. *Physiol. Rev.* 81, 741–766.

(24) Gu, Y., Luchsinger, J. A., Stern, Y., and Scarmeas, N. (2010) Mediterranean diet, inflammatory and metabolic biomarkers, and risk of Alzheimer's disease. *J. Alzheimers Dis* 22, 483–492.

(25) Gardener, S., Gu, Y., Rainey-Smith, S. R., Keogh, J. B., Clifton, P. M., Mathieson, S. L., Taddei, K., Mondal, A., Ward, V. K., Scarmeas, N., Barnes, M., Ellis, K. A., Head, R., Masters, C. L., Ames, D., Macaulay, S. L., Rowe, C. C., Szoek, C., and Martins, R. N. (2012) Adherence to a Mediterranean diet and Alzheimer's disease risk in an Australian population. *Transl. Psychiatry* 2, e164.

(26) Haass, C., and Selkoe, D. J. (2007) Soluble protein oligomers in neurodegeneration: lessons from the Alzheimer's amyloid beta-peptide. *Nat. Rev. Mol. Cell Biol.* 8, 101–112.

(27) Reilly, J. F., Games, D., Rydel, R. E., Freedman, S., Schenk, D., Young, W. G., Morrison, J. H., and Bloom, F. E. (2003) Amyloid deposition in the hippocampus and entorhinal cortex: quantitative analysis of a transgenic mouse model. *Proc. Natl. Acad. Sci. U. S. A.* 100, 4837–4842.

(28) Davis, J., Xu, F., Deane, R., Romanov, G., Previti, M. L., Zeigler, K., Zlokovic, B. V., and Van Nostrand, W. E. (2004) Early-onset and robust cerebral microvascular accumulation of amyloid beta-protein in transgenic mice expressing low levels of a vasculotropic Dutch/Iowa mutant form of amyloid beta-protein precursor. *J. Biol. Chem.* 279, 20296–20306.

(29) Zhang-Nunes, S. X., Maat-Schieman, M. L., van Duinen, S. G., Roos, R. A., Frosch, M. P., and Greenberg, S. M. (2006) The cerebral beta-amyloid angiopathies: hereditary and sporadic. *Brain Pathol.* 16, 30–39.

(30) Haass, C. (2004) Take five–BACE and the gamma-secretase quartet conduct Alzheimer's amyloid beta-peptide generation. *EMBO J.* 23, 483–488.

(31) Selkoe, D. J. (1993) Physiological production of the beta-amyloid protein and the mechanism of Alzheimer's disease. *Trends Neurosci.* 16, 403–409.

(32) Sisodia, S. S., Koo, E. H., Beyreuther, K., Unterbeck, A., and Price, D. L. (1990) Evidence that beta-amyloid protein in Alzheimer's disease is not derived by normal processing. *Science* 248, 492–495.

(33) Bell, R. D., and Zlokovic, B. V. (2009) Neurovascular mechanisms and blood-brain barrier disorder in Alzheimer's disease. *Acta Neuropathol.* 118, 103–113.

(34) Deane, R., Wu, Z., Sagare, A., Davis, J., Du Yan, S., Hamm, K., Xu, F., Parisi, M., LaRue, B., Hu, H. W., Spijkers, P., Guo, H., Song, X., Lenting, P. J., Van Nostrand, W. E., and Zlokovic, B. V. (2004) LRP/amyloid beta-peptide interaction mediates differential brain efflux of A β isoforms. *Neuron* 43, 333–344.

(35) Wang, Y. J., Zhou, H. D., and Zhou, X. F. (2006) Clearance of amyloid-beta in Alzheimer's disease: progress, problems and perspectives. *Drug Discovery Today* 11, 931–938.

(36) Qosa, H., Abuasal, B. S., Romero, I. A., Weksler, B., Couraud, P. O., Keller, J. N., and Kaddoumi, A. (2014) Differences in amyloid-beta clearance across mouse and human blood-brain barrier models: Kinetic analysis and mechanistic modeling. *Neuropharmacology* 79C, 668–678.

(37) Cirrito, J. R., Deane, R., Fagan, A. M., Spinner, M. L., Parsadanian, M., Finn, M. B., Jiang, H., Prior, J. L., Sagare, A., Bales, K. R., Paul, S. M., Zlokovic, B. V., Pivnicka-Worms, D., and Holtzman, D. M. (2005) P-glycoprotein deficiency at the blood-brain barrier increases amyloid-beta deposition in an Alzheimer disease mouse model. *J. Clin. Invest.* 115, 3285–3290.

(38) Shibata, M., Yamada, S., Kumar, S. R., Calero, M., Bading, J., Frangione, B., Holtzman, D. M., Miller, C. A., Strickland, D. K., Ghiso, J., and Zlokovic, B. V. (2000) Clearance of Alzheimer's amyloid-beta(1–40) peptide from brain by LDL receptor-related protein-1 at the blood-brain barrier. *J. Clin. Invest.* 106, 1489–1499.

(39) Qosa, H., Abuznait, A. H., Hill, R. A., and Kaddoumi, A. (2012) Enhanced brain amyloid-beta clearance by rifampicin and caffeine as a possible protective mechanism against Alzheimer's disease. *J. Alzheimers Dis* 31, 151–165.

(40) Kline, A. (2012) Apolipoprotein E, amyloid-ss clearance and therapeutic opportunities in Alzheimer's disease. *Alzheimer's Res. Ther.* 4, 32.

(41) Wildsmith, K. R., Holley, M., Savage, J. C., Skerrett, R., and Landreth, G. E. (2013) Evidence for impaired amyloid beta clearance in Alzheimer's disease. *Alzheimer's Res. Ther.* 5, 33.

(42) Chawla, A., Boisvert, W. A., Lee, C. H., Laffitte, B. A., Barak, Y., Joseph, S. B., Liao, D., Nagy, L., Edwards, P. A., Curtiss, L. K., Evans, R. M., and Tontonoz, P. (2001) A PPAR gamma-LXR-ABCA1 pathway in macrophages is involved in cholesterol efflux and atherogenesis. *Mol. Cell* 7, 161–171.

(43) Zolezzi, J. M., Bastias-Candia, S., Santos, M. J., and Inestrosa, N. C. (2014) Alzheimer's disease: relevant molecular and physiopathological events affecting amyloid-beta brain balance and the putative role of PPARs. *Front. Aging Neurosci.* 6, 176.

(44) Cramer, P. E., Cirrito, J. R., Wesson, D. W., Lee, C. Y., Karlo, J. C., Zinn, A. E., Casali, B. T., Restivo, J. L., Goebel, W. D., James, M. J., Brunden, K. R., Wilson, D. A., and Landreth, G. E. (2012) ApoE-directed therapeutics rapidly clear beta-amyloid and reverse deficits in AD mouse models. *Science* 335, 1503–1506.

(45) Kim, H. J., Moon, J. H., Kim, H. M., Yun, M. R., Jeon, B. H., Lee, B., Kang, E. S., Lee, H. C., and Cha, B. S. (2014) The hypolipidemic effect of cilostazol can be mediated by regulation of hepatic low-density lipoprotein receptor-related protein 1 (LRP1) expression. *Metab., Clin. Exp.* 63, 112–119.

(46) Rocejanasaroj, A., Tencomnao, T., and Sangkitikomol, W. (2014) Thunbergia laurifolia extract minimizes the adverse effects of toxicants by regulating P-glycoprotein activity, CYP450, and lipid metabolism gene expression in HepG2 cells. *GMR, Genet. Mol. Res.* 13, 205–219.

(47) Lefebvre, P., Benomar, Y., and Staels, B. (2010) Retinoid X receptors: common heterodimerization partners with distinct functions. *Trends Endocrinol. Metab.* 21, 676–683.

(48) Iqbal, K., Liu, F., Gong, C. X., Alonso, A. C., and Grundke-Iqbal, I. (2009) Mechanisms of tau-induced neurodegeneration. *Acta Neuropathol.* 118, 53–69.

(49) Alonso, A. D., Di Clerico, J., Li, B., Corbo, C. P., Alaniz, M. E., Grundke-Iqbal, I., and Iqbal, K. (2010) Phosphorylation of tau at Thr212, Thr231, and Ser262 combined causes neurodegeneration. *J. Biol. Chem.* 285, 30851–30860.

(50) Oddo, S., Billings, L., Kesslak, J. P., Cribbs, D. H., and LaFerla, F. M. (2004) A β immunotherapy leads to clearance of early, but not late, hyperphosphorylated tau aggregates via the proteasome. *Neuron* 43, 321–332.

(51) Sofroniew, M. V. (2015) Astrogliosis. *Cold Spring Harbor Perspect. Biol.* 7, a020420.

(52) Verkhratsky, A., Rodríguez, J. J., and Steardo, L. (2014) Astroglipathology: a central element of neuropsychiatric diseases? *Neuroscientist* 20, 576–588.

(53) Heppner, F. L., Ransohoff, R. M., and Becher, B. (2015) Immune attack: the role of inflammation in Alzheimer disease. *Nat. Rev. Neurosci.* 16, 358–372.

(54) Tong, L., Balazs, R., Soiapornkul, R., Thangnipon, W., and Cotman, C. W. (2008) Interleukin-1 beta impairs brain derived neurotrophic factor-induced signal transduction. *Neurobiol. Aging* 29, 1380–1393.

(55) Fuller, S., Steele, M., and Münch, G. (2010) Activated astroglia during chronic inflammation in Alzheimer's disease-do they neglect their neurosupportive roles? *Mutat. Res., Fundam. Mol. Mech. Mutagen.* 690, 40–49.

(56) Brahmachari, S., Fung, Y. K., and Pahan, K. (2006) Induction of glial fibrillary acidic protein expression in astrocytes by nitric oxide. *J. Neurosci.* 26, 4930–4939.

(57) Iacono, A., Gómez, R., Sperry, J., Conde, J., Bianco, G., Meli, R., Gómez-Reino, J. J., Smith, A. B., 3rd, and Gualillo, O. (2010) Effect of oleocanthal and its derivatives on inflammatory response induced by lipopolysaccharide in a murine chondrocyte cell line. *Arthritis Rheum.* 62, 1675–1682.

(58) Elnagar, A. Y., Sylvester, P. W., and El Sayed, K. A. (2011) (-)-Oleocanthal as a c-Met inhibitor for the control of metastatic breast and prostate cancers. *Planta Med.* 77, 1013–1019.

(59) Ly, P. T., Cai, F., and Song, W. (2011) Detection of neuritic plaques in Alzheimer's disease mouse model. *J. Visualized Exp.* 53, e2831.

(60) Zinchuk, V., Zinchuk, O., and Okada, T. (2007) Quantitative colocalization analysis of multicolor confocal immunofluorescence microscopy images: pushing pixels to explore biological phenomena. *Acta Histochem. Cytochem.* 40, 101–111.

(61) Pacheco-Quinto, J., and Eckman, E. A. (2013) Endothelin-converting enzymes degrade intracellular beta-amyloid produced within the endosomal/lysosomal pathway and autophagosomes. *J. Biol. Chem.* 288, 5606–5615.